



## Article

# Long-Term Efficacy of Poly(L-lactide-co- $\epsilon$ -caprolactone) Copolymer Lifting Threads with Encapsulated MICROscale Hyaluronic Acid Particles Using NAMICA Technology: Investigating Biorevitalizing Effects in Skin Remodeling (Part 1)

Pavel Burko <sup>1,\*</sup> , George Sulamanidze <sup>2</sup> and Dmitriy Nikishin <sup>3</sup> 

<sup>1</sup> Section of Human Anatomy, Department of Biomedicine, Neurosciences and Advanced Diagnostics (BiND), University of Palermo, Via del Vespro, 129, 90127 Palermo, PA, Italy

<sup>2</sup> Headquarter of the APTOS LLC, G. Amilakhvari Str., 15, 0109 Tbilisi, Georgia; aptos@aptos.ge

<sup>3</sup> Russian Office of the APTOS LLC, Territory of Skolkovo Innovation Center, Bolshoy Boulevard, 42, Building 1, Rooms 873 and 885, 121205 Moscow, Russia; d.nikishin@aptos.group

\* Correspondence: pavel.burko@unipa.it; Tel.: +39-3517925335

**Abstract:** Facial thread lifting with absorbable threads such as poly(L-lactide-co- $\epsilon$ -caprolactone) (P(LA/CL)) has been explored in an animal model. This experimental study utilized P(LA/CL)-HA-micro threads enhanced with hyaluronic acid microencapsulation via NAMICA technology in five four-month-old female pigs. The effects were compared to those of P(LA/CL)-HA threads over a six-month period through histological analysis. The results indicated improvements in skin remodeling, with P(LA/CL)-HA-micro threads enabling controlled and prolonged release of hyaluronic acid, leading to sustained improvements in tissue structure. These findings suggest that microencapsulated threads could enhance therapeutic outcomes; however, these results are preliminary and derived from an animal model. Further research and clinical trials are necessary to confirm these benefits in human subjects.



Academic Editor: Vasil Georgiev

Received: 25 December 2024

Revised: 18 January 2025

Accepted: 21 January 2025

Published: 23 January 2025

**Citation:** Burko, P.; Sulamanidze, G.; Nikishin, D. Long-Term Efficacy of Poly(L-lactide-co- $\epsilon$ -caprolactone) Copolymer Lifting Threads with Encapsulated MICROscale Hyaluronic Acid Particles Using NAMICA Technology: Investigating Biorevitalizing Effects in Skin Remodeling (Part 1). *Cosmetics* **2025**, *12*, 20. <https://doi.org/10.3390/cosmetics12010020>

**Copyright:** © 2025 by the authors. Licensee MDPI, Basel, Switzerland. This article is an open access article distributed under the terms and conditions of the Creative Commons Attribution (CC BY) license (<https://creativecommons.org/licenses/by/4.0/>).

**Keywords:** biorevitalization; non-surgical facelift; hyaluronic acid; skin remodeling; lifting threads

## 1. Introduction

Facial thread lifting is recognized as a minimally invasive technique characterized by notable aesthetic results. Traditionally, this procedure is associated with few significant complications, which highlights its perceived safety and efficacy [1,2]. However, recent comprehensive meta-analyses, including a study by Niu Z. et al. (2021) [2], suggest that complications, while generally infrequent, do occur at notable rates. This meta-analysis, which reviewed 26 studies, revealed the following complication rates: swelling (35%), skin dimpling (10%), paresthesia (6%), thread visibility or palpability (4%), infection (2%), and thread extrusion (2%). Importantly, the type of thread used significantly influences complication rates; compared with non-absorbable threads, absorbable threads are associated with a significantly lower risk of paresthesia (3.1% vs. 11.7%) and thread extrusion (1.6% vs. 7.6%). Additionally, age appears to be a critical factor in the risk profile; patients older than 50 years experienced higher rates of skin dimpling (16% vs. 5.6%) and infection (5.9% vs. 0.7%) than their younger counterparts did. These findings underscore the necessity of careful patient selection and technique customization to minimize adverse outcomes [3].

Considering the intricacies involved, the utilization of ultrasonography (US) is becoming increasingly indispensable in enhancing the accuracy and safety of minimally invasive cosmetic interventions, such as thread lifting. Ultrasonography, which is renowned for its non-invasive, dynamic, and cost-efficient characteristics, enables real-time imaging crucial for the precise placement of sutures, thereby minimizing the likelihood of adverse events. Furthermore, ultrasonography facilitates a thorough evaluation of dermal thickness, volume augmentation, and vascular architecture, including the application of color Doppler US to monitor hemodynamic changes associated with inflammation, thus assisting in the prevention and management of potential complications [4,5].

At present, absorbable threads are made from biodegradable synthetic polymers such as polydioxanone (PDO) or poly-p-dioxanone (PPDO), polyglycolic acid (PGA), poly-L-lactic acid (PLLA), polylactic acid-caprolactone (PLACL), polylactic-co-glycolic acid (PLGA), and poly( $\epsilon$ -caprolactone) (PCL) [6–9]. Recently, the field has expanded to incorporate poly(L-lactide-co- $\epsilon$ -caprolactone) (P(LA/CL)), a copolymer derived from L-lactic acid (LA) and  $\epsilon$ -caprolactone (CL) [10]. This material is utilized across several areas of tissue engineering, regenerative medicine, and aesthetic medicine. It has high biocompatibility, safety, and tolerability, making it ideal for uses that demand extended performance owing to its slower degradation pace [11–13]. The degradation timeline for these threads generally ranges from 9 to 12 months, offering sufficient support for tissue remodeling and potentially prolonging the lifting effect [14]. Clinical research indicates that the effects of P(LA/CL) threads may extend beyond 18 months because their collagen-stimulating properties are improved compared to those of earlier generations [13].

As the field of aesthetic medicine has evolved swiftly, addressing the notable gap in predictive effectiveness is essential. In choosing threads for facial thread lifting, it is crucial to evaluate not only their capacity for an immediate lifting effect but also their role in facilitating structural skin remodeling. The absence of biorevitalizing properties in these threads could curtail the long-term success of lifting procedures, possibly failing to fulfil the expectations of aesthetic medicine practitioners and their patients. To improve therapeutic outcomes, thread lifting is often paired with hyaluronic acid injections, which have been proven to improve clinical results [15,16]. Using a synergistic approach, APTOS LLC (Tbilisi, Georgia) was developed by developing hyaluronic acid-coated threads designed to streamline the lifting process and reduce adverse effects following the procedure, thereby improving overall patient outcomes [6,17,18].

NAMICA encapsulation technology, developed by APTOS LLC (Tbilisi, Georgia), introduces a method for the extended release of hyaluronic acid through medical implants. This patented technique [17] starts by mixing medium molecular weight, non-crosslinked sodium hyaluronate at 2 wt% of the total mass with isopropyl alcohol at 98 wt% of the total mass. This process creates an emulsion, which serves as the foundation. To this base, an organic solvent, along with a copolymer (balanced mixture of PLLA and/or poly-D-lactic acid (PDLA) in a 1:1 ratio), is added. This mixture is then uniformly applied to the surface of lifting threads by electrospinning over a period of 60 s, resulting in a consistent coating that is 10 microns thick.

This coating comprises polymer microfibers embedded with polysaccharide microcapsules, ranging in size from 1 to 30 microns (Figure 1). It is designed for the gradual release of HA, as assessed via an assay that utilizes high-performance liquid chromatography (HPLC). This methodology provides precise measurements of the microcapsule dissolution rates, enabling the evaluation of the release kinetics of the embedded active substances. The assay is conducted under simulated physiological conditions using phosphate-buffered saline (PBS) at a pH of 7.4 to mimic the body's environment. This setup ensures that the performance of the coating in terms of gradual substance release can be accurately

monitored over specified time intervals, providing data for optimizing the therapeutic efficacy and application timing of the coated implants.

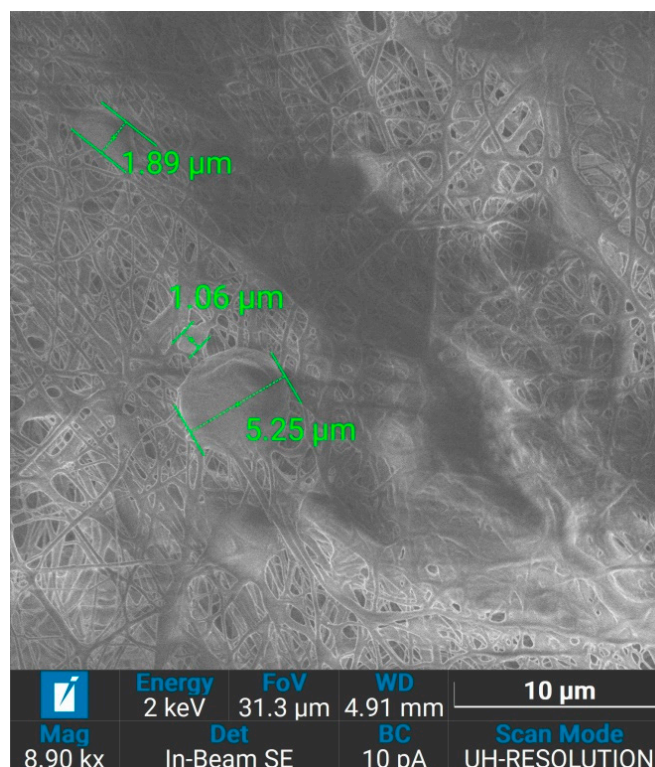


**Figure 1.** This illustration depicts the surface topography of the P(LA/CL)-HA-micro thread, as observed through scanning electron microscopy (SEM) at a magnification of 8900 $\times$ . The image reveals three measured microcapsules embedded within the microfibers of the copolymer matrix. The acquisition was executed via an in-beam secondary electron detector, employing a beam energy of 2 keV and a beam current of 10 pA, configured to ultrahigh-resolution scanning mode. With a field of view measuring 31.3  $\mu\text{m}$  and a working distance of 4.91 mm, the setup facilitated an intricate depiction of the microstructural elements.

The copolymerization of lactide with  $\epsilon$ -caprolactone effectively modulates the mechanical properties, shape-memory capabilities, degradation kinetics, and controlled drug-release properties of PLLA, enhancing its biomedical applications. Synthesization through ring-opening polymerization (ROP), P(LA/CL) allows precise control over its characteristics by adjusting the molar ratios of L-lactic acid (LA) and  $\epsilon$ -caprolactone (CL) and the polymerization duration, which is typically optimized at a 1:1 LA to CL ratio over 30 h [11,19].

These parameters influence the copolymer's molecular weight, polydispersity, and glass transition temperature, which exhibit an augmentation correlating with the elevated levels of LA content. Mechanically, P(LA/CL) exhibits superior toughness and elasticity, making it suitable for dynamic biomedical uses. Its biodegradability and bioabsorbability further support its use in medical applications requiring temporary structural support [11].

The beneficial effects of P(LA/CL) threads on the production of collagen, which is essential for skin rejuvenation, are well established in the scientific literature [13]. Nevertheless, it is crucial to acknowledge that a comprehensive assessment of structural skin remodeling needs to go beyond merely evaluating the effects on collagen production. An in-depth evaluation should also account for the thread's specific effects on stimulating type I and III collagen, promoting elastogenesis, modifying the cellular composition, and affecting the morphometric properties of vessels. Moreover, a detailed morphological assessment might necessitate the examination of additional parameters to fully understand the extent and effectiveness of the intervention.

In our experimental study, we evaluated the long-term efficacy of lifting threads produced by Aptos LLC (Tbilisi, Georgia) [17], which are composed of P(LA/CL) embedded with encapsulated microscale hyaluronic acid particles via NAMICA technology (P(LA/CL)-HA-micro). This advanced approach capitalizes on the ability of P(LA/CL) to deliver hyaluronic acid in a controlled and sustained manner, aiming to enhance therapeutic outcomes in tissue rejuvenation and improve skin structure. By integrating NAMICA technology, the threads provide a precise release profile of hyaluronic acid, optimizing its bioavailability and maximizing the functional benefits over an extended period. The primary goal of this research was to assess and compare the effectiveness of the P(LA/CL)-HA-micro formulation with that of traditional P(LA/CL)-HA formulations over a six-month period, particularly with respect to their impact on skin remodeling. This study highlights the potential of microscale HA encapsulation to significantly enhance the performance and durability of medical implants, underscoring its advantages in improving aesthetic outcomes.

## 2. Materials and Methods

The inclusion criteria for utilizing the porcine model were as follows:

1. Breed: Large White;
2. Age: Four months;
3. Weight: Commencing at 40 kg;
4. Health: The pigs must be in optimal health and devoid of any discernible diseases or abnormalities;
5. Gender: Female;
6. Housing: There should be a one-week acclimatization period prior to the commencement of the study.

The exclusion criteria for utilizing the porcine model were as follows:

1. Health: Any pigs demonstrating symptoms of illness, injuries, or other health complications were excluded.
2. Reproductive Status: Female pigs that are pregnant or currently lactating are not eligible.
3. Prior Research Involvement: Pigs previously utilized in experimental procedures are precluded from participation.

The research involved five 4-month-old female pigs of the Large White breed, each weighing 40 kg at the start of the study. These animals were housed under conditions optimized for their well-being, with temperatures maintained at  $21 \pm 2$  °C, relative humidity between 30–60%, and a light/dark cycle of 12 h each starting at 7 AM. Food and water were available to them at all times. Following a one-week acclimatization period, the pigs were randomly assigned numbers.

The procedure for thread placement was conducted under both inhalational and intravenous anesthesia in a sterile surgical environment. The investigation employed systemic analgesics routinely utilized in both veterinary and clinical settings. The standardization of anesthesia induction across all subjects involved the administration of 6 mL of xylazine and 0.7 mL of zoletil 100, both of which were delivered intramuscularly. This protocol facilitated the catheterization of the external auricular vein via a 22 G catheter, which was essential for subsequent interventions. To sustain the anesthetic plane, intermittent intravenous administration of 4 mL of propofol at 20 min intervals was implemented.

During the intraoperative phase, anesthesia was maintained with a 3.0 vol% concentration of isoflurane administered via mask inhalation for three minutes. Further maintenance of anesthesia involved the use of a Dräger Fabius Plus anesthesia machine

(Berlin, Germany) to deliver a gaseous mixture containing 65–70% oxygen and 1.5 vol% isoflurane. Additionally, propofol was continuously infused at a rate of 25 mL/h.

Prophylactic measures to prevent postoperative complications included the administration of 1.0 mL of ceftriaxone intramuscularly once. Intraoperative monitoring parameters included heart rate, arterial pressure, and pulse oximetry. Recovery from anesthesia was typically observed within 30–40 min following the cessation of propofol infusion and discontinuation of the inhalational anesthetic agent.

Prior to surgery, the surgical sites on the torso and limbs (both forelimbs and hindlimbs) were shaved and disinfected with 70% alcohol. Using an 18 G straight needle, five threads of each type were implanted into the subcutaneous layer of each pig, oriented parallel to the skin surface. Access was gained on the right side via 5 puncture points where 5 units of absorbable P(LA/CL)-HA threads (produced by APTOS LLC (Tbilisi, Georgia)) were implanted. Similarly, on the left side, 5 puncture points were used for the implantation of 5 units of P(LA/CL)-HA-micro threads from the same manufacturer. The access points were subsequently sealed with aseptic stickers. All threads used were 15 cm in length, non-barbed, and USP 2–0 in size. The surgical procedures were carried out successfully without any complications.

Following the implantation of the lifting threads, samples of skin along with subcutaneous tissue were collected at 5 distinct time points: 7, 21, 30, 90, and 180 days. A 15 cm segment of soft tissue was surgically removed, from which three specimens were harvested for detailed histological evaluation—one from each extremity and one from the median section (Figure S1). Untreated skin from nearby areas served as a control. Each pig was subjected to the same procedural sequence at intervals of 1 week, 21 days, 1 month, 3 months, and 6 months post-reading to analyze the effects systematically.

Post-experiment euthanasia was administered through an intravenous overdose of xylazine and zoletil 100, culminating in exsanguination once profound drug-induced sleep was attained.

Tissue samples were preserved by fixing them in 7% neutral buffered formalin for 24 h, effectively stopping the biochemical processes within the tissues. After fixation, the biopsy samples were dehydrated through a graded alcohol series and then permeated with organic solvents prior to being encased in hot liquid paraffin. As the paraffin solidified upon cooling, it provided essential structural support to the tissues. These prepared samples were subsequently cut into full-thickness slices of 5–7 microns using a microtome. A minimum of three sections from each sample were transferred to glass slides for microscopic evaluation. The sections were then dewaxed and stained via three different procedures: (1) hematoxylin and eosin (H&E), (2) Weigert-Van Gieson, and (3) Sirius Red staining. Each staining method was selected to highlight different tissue components for detailed histological analysis. A digital microscope equipped with a 12 MP Sony sensor was used to analyze the stained tissue sections via both light microscopic observation and polarized light microscopy. During these examinations, the image capture technique involved taking five images at 40× magnification from each glass slide, ten images at 100× magnification from each glass slide (five from the dermis and five from the hypodermis), and ten images at 200× magnification from each glass slide (five from the dermis and five from the hypodermis). Morphological assessments focused on various parameters, including the cellular composition, dermal thickness, thickness of the fibrous sheath, and morphometric properties of the vessels, such as the blood vessel diameter, relative area of the vascular bed, and fibrocyte count. Additional evaluations included measuring the collagen density, quantity of type I and III collagen, ratio of type I to III collagen, and elastin levels in the dermis and hypodermis. These analyses were conducted via the software programs ImageView v.3.7.7 and HistMorph v.2.3 to ensure precise and detailed evaluations.



Statistical calculations were conducted via the Statistica v.7 software package. Initially, descriptive statistics were computed, which included the calculation of mean values with standard errors ( $M \pm m$ ), medians, and quartiles (25% and 75%), as well as recording the minimum and maximum values for each day studied and across all days (as detailed in Tables S1–S3). The next phase of the statistical analysis focused on the day-to-day dynamics of each parameter for each type of thread separately. Comparisons of the data were made via nonparametric methods, specifically the Wilcoxon test for related samples. The results were deemed statistically significant at  $p < 0.05$ , with a trend toward significance indicated by  $0.05 < p < 0.1$ , suggesting that further significance could be established with a larger sample size. Finally, comparative analyses were performed via the Wilcoxon test to compare the effects of the two types of threads against each other and the control across the individual and combined study days.

### 3. Results

#### 3.1. Tissue Changes Due to P(LA/CL)-HA-Micro Threads

In our study assessing the impact of P(LA/CL)-HA-micro threads over time, we utilized the Wilcoxon test within our statistical analysis to detect shifts across different time intervals (Figure 2). This method established a strong framework for analyzing the dynamic nature and effectiveness of the tissue responses induced by threads.

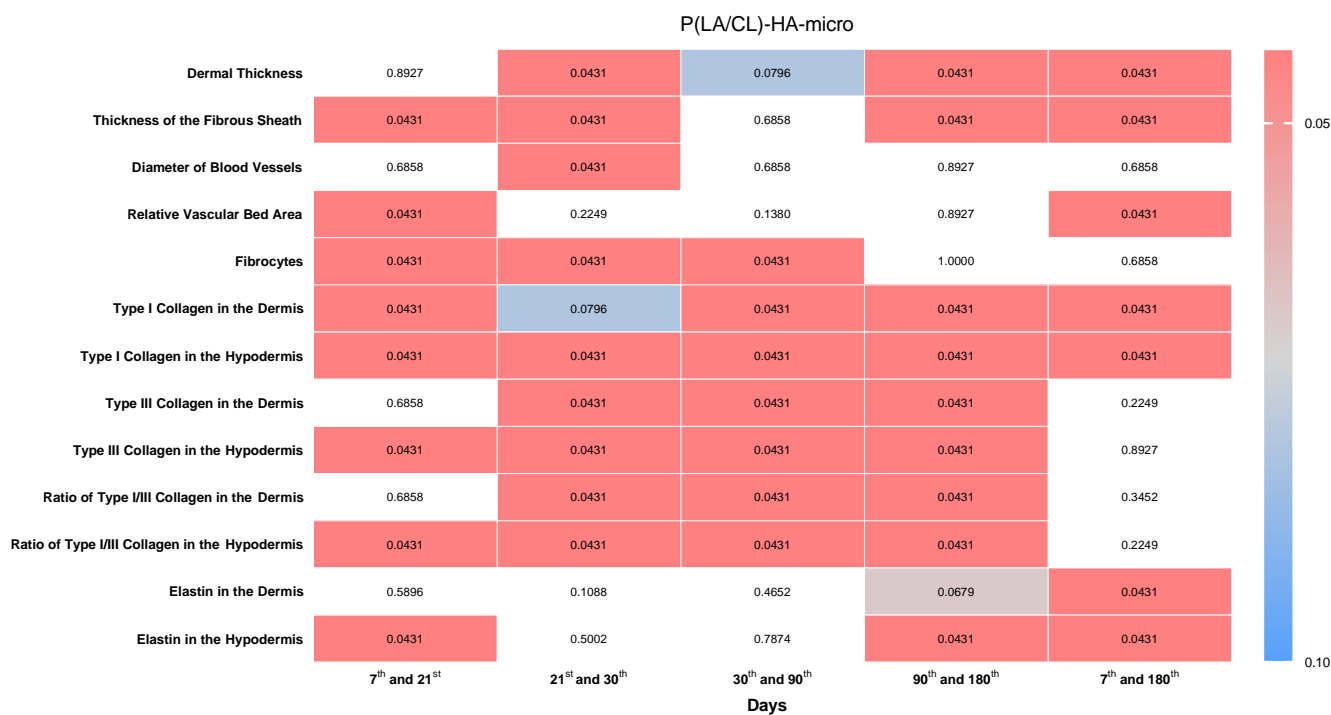


**Figure 2.** The heatmap visually displays the data spanning various indicators and time intervals for P(LA/CL)-HA-micro threads. The color intensity within each cell correlates with the  $p$ -value, which graphically illustrates the significance levels at specific points. The results with a  $p$ -value less than 0.05 were deemed statistically significant, and values between 0.05 and 0.1 suggested a trend toward significance, implying that further analysis with more samples might confirm these findings. Cells without color represent  $p$ -values that do not fall within these specified ranges.

For dermal thickness, statistically significant changes were observed between 21 and 30 days and between 90 and 180 days. Additionally, a trend towards a statistically significant difference was noted between 30 and 90 days.

With respect to the metric thickness of the fibrous sheath, significant changes were identified between 7 and 21 days, 21 and 30 days, and 90 and 180 days (no significant differences were observed between 30 and 90 days).

The diameter of the blood vessels significantly changed only between 21 and 30 days, whereas the relative vascular bed area significantly changed only between 7 and 21 days.

Compared with those on day 7, the number of fibrocytes on day 21 was significantly lower, the fibrocyte count on day 30 was significantly greater than that on day 21, and the number of fibrocytes on day 90 was significantly lower, returning nearly to baseline levels, with no significant changes by day 180.

Statistically significant differences were observed across all time intervals for type I collagen density, type III collagen density, and the ratio of type I/III collagen in the hypodermis. Conversely, for the dermis, changes in type I collagen density, type III collagen density, and the ratio of type I/III collagen were not statistically significant between 21 and 30 days, although a trend toward significance was observed for type I collagen density. No significant differences in type III collagen density and the ratio of type I/III collagen in the dermis were noted between 7 and 21 days.

For elastin density in the dermis, no significant differences were observed except for a trend toward significance at 90 and 180 days. In the hypodermis, elastin density significantly changed between 7 and 21 days and between 90 and 180 days.

Statistically significant differences between initial (day 7) and final (day 180) values were noted for dermal thickness, thickness of the fibrous sheath, relative vascular bed area, type I collagen in both the dermis and hypodermis, and elastin density in both the dermis and hypodermis.

### 3.2. Comparative Analysis of the P(LA/CL)-HA-Micro Threads Versus P(LA/CL)-HA Threads, and P(LA/CL)-HA-Nano Threads Versus Control on Various Histological Indicators

A comparative analysis via the Wilcoxon test was performed between two types of threads, P(LA/CL)-HA-micro and P(LA/CL)-HA. This analysis included comparisons both between the thread types and against a control group, conducted for each individual day of the study as well as cumulatively across all days (Figures 3 and 4).

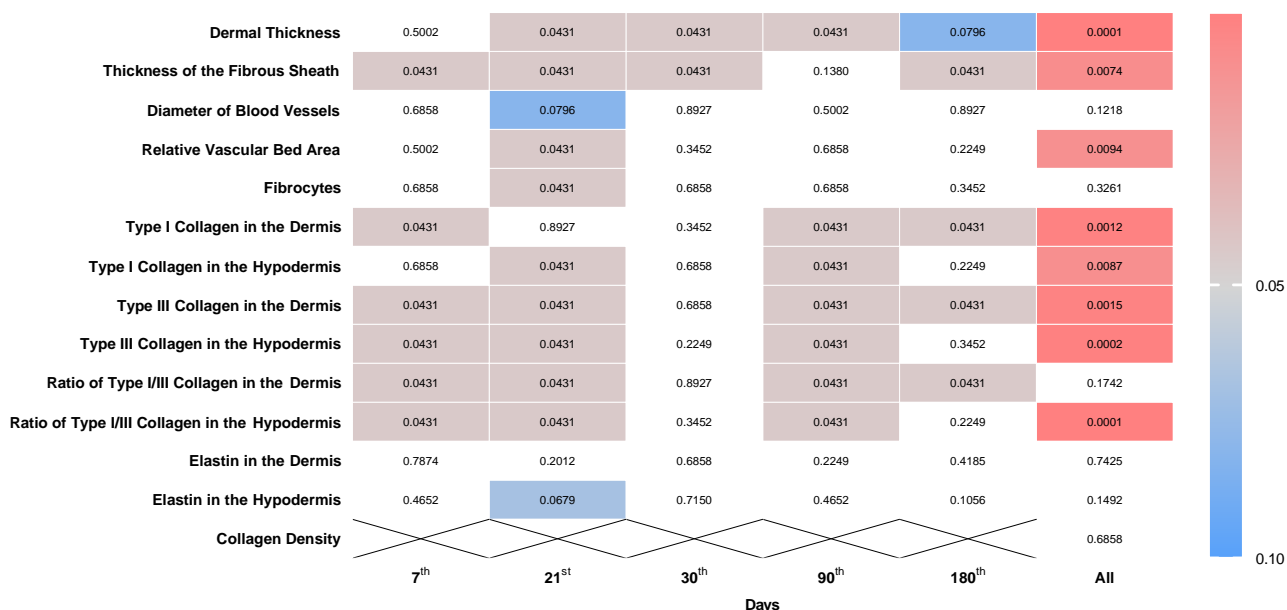
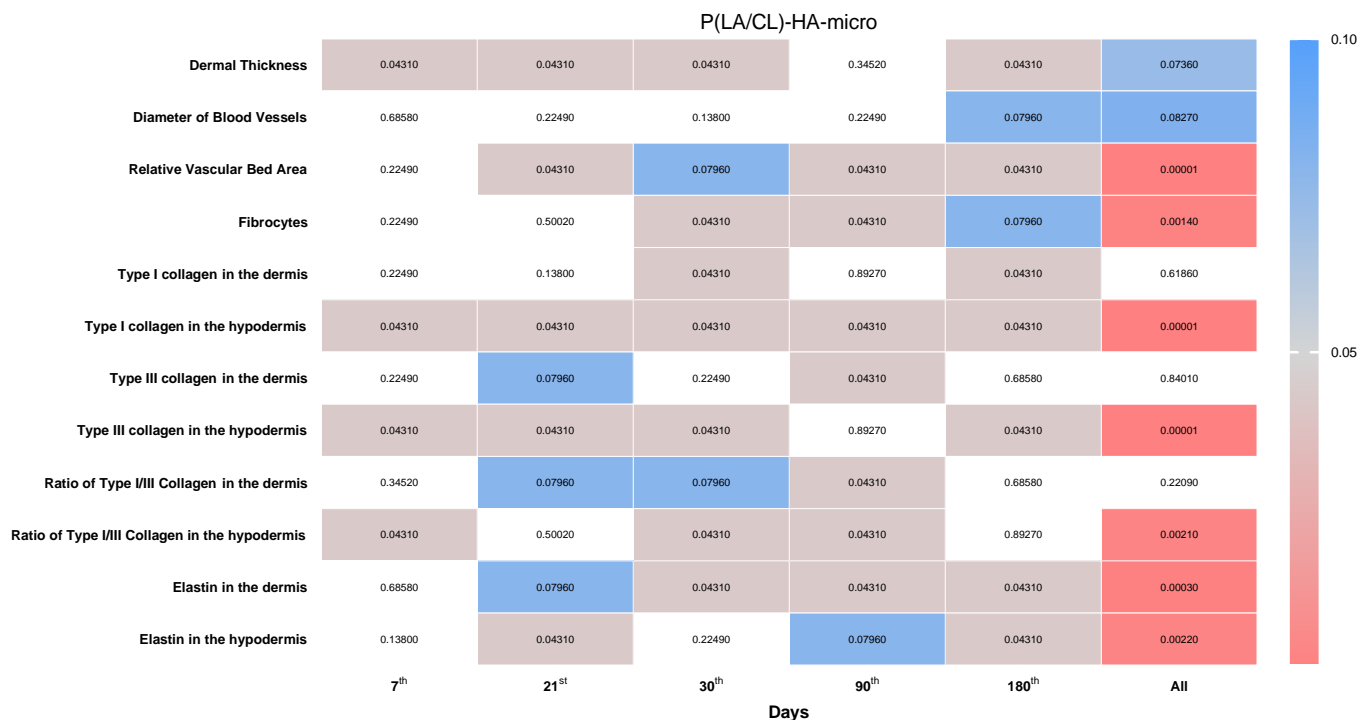


Figure 3. The heatmap visualizes data across various indicators and days, comparing P(LA/CL)-HA-micro and P(LA/CL)-HA threads. The color intensity in each cell reflects the p-value, serving as a visual cue to the significance levels at different points. Outcomes with a p-value less than 0.05 were

deemed statistically significant, whereas a *p*-value between 0.05 and 0.1 indicated a potential trend toward significance, suggesting that additional sampling could affirm these differences. Cells without color represent *p*-values that do not meet the criteria for significance.



**Figure 4.** The heatmap shows data for various indicators over different days, comparing P(LA/CL)-HA-micro threads against a control, assessed separately for each thread type. The intensity of color in each cell correlates with the *p*-value, which visually encodes the levels of statistical significance at specific data points. The results with a *p*-value less than 0.05 were classified as statistically significant. A *p*-value between 0.05 and 0.1 suggested a potentially significant difference, implying that increasing the sample size could confirm these initial findings. Cells lacking color represent *p*-values that fall outside these defined significance thresholds.

According to the data collected, the use of P(LA/CL)-HA-micro and P(LA/CL)-HA threads resulted in statistically significant differences in the majority of the indicators on various days of the study. No significant differences were observed in the diameter of blood vessels, elastin density in the dermis and hypodermis, and collagen density.

### 3.2.1. Dermal Thickness

*P(LA/CL)-HA-micro vs. Control.* The dermal thickness when P(LA/CL)-HA-micro threads were used was consistently lower than the control values from day 7 to day 90, with statistically significant differences observed on days 7, 21, and 30. However, by day 180, there was a substantial increase in this indicator, resulting in the values for P(LA/CL)-HA-micro threads becoming significantly greater than those of the control.

*P(LA/CL)-HA-micro vs. P(LA/CL)-HA.* Throughout the study period, the dermal thickness when P(LA/CL)-HA threads were used consistently exceeded the values observed with P(LA/CL)-HA-micro threads. Statistically significant differences were noted on days 21, 30, and 90. By day 180, there was a trend indicating the potential emergence of a statistically significant difference.

The histological data on dermal thickness are graphically presented in Figures 5 and S2.



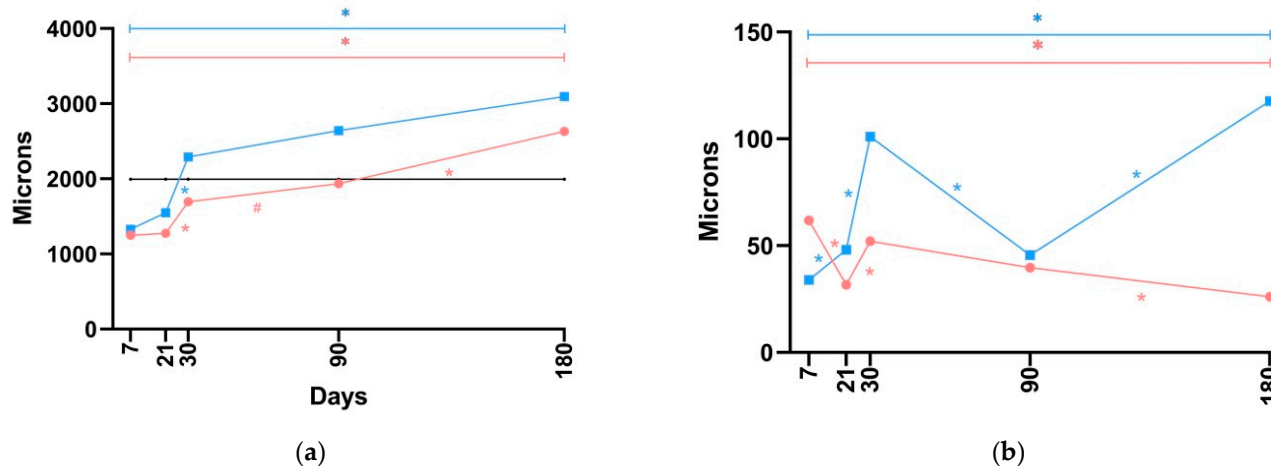


**Figure 5.** The linear graphs present data on dermal thickness (a) and fibrous sheath thickness (b) over five time points during the post-implantation assessment, based on median values. In these graphs, the control group is denoted in black, P(LA/CL)-HA is in blue, and P(LA/CL)-HA-micro is in red. The results that reached a  $p$ -value less than 0.05 were deemed statistically significant, marked with an asterisk (\*) for  $0.01 \leq p < 0.05$ , and a hash sign (#) marks a  $p$ -value between 0.05 and 0.1, suggesting a trend toward significance that could be confirmed with a larger sample size.

### 3.2.2. Thickness of the Fibrous Sheath

*P(LA/CL)-HA-micro* vs. *P(LA/CL)-HA*. Throughout the study period, except on day 90, the thickness of the fibrous sheath significantly differed when P(LA/CL)-HA and P(LA/CL)-HA-micro threads were used. Notably, on day 7, this metric was significantly greater with P(LA/CL)-HA-micro than with P(LA/CL)-HA, whereas on all other days, the opposite was observed, with higher values recorded when P(LA/CL)-HA was used.

The histological data related to the thickness of the fibrous sheath are graphically illustrated in Figures 5 and S3.

### 3.2.3. Diameter of Blood Vessels

*P(LA/CL)-HA-micro* vs. *Control*. The values of the diameter of blood vessels when P(LA/CL)-HA-micro was used were below the control values on days 7 and 21. Conversely, on days 30, 90, and 180, the values were greater than those of the controls with P(LA/CL)-HA-micro, with a trend toward a statistically significant difference noted on day 180.

*P(LA/CL)-HA-micro* vs. *P(LA/CL)-HA*. Regarding the diameter of blood vessels, as noted earlier, no statistically significant differences were observed. Importantly, this parameter, when P(LA/CL)-HA was used, exceeded the corresponding values of P(LA/CL)-HA-micro on days 7, 21, and 90, whereas on days 30 and 180, the values were greater for P(LA/CL)-HA-micro. A trend towards a statistically significant difference was observed on day 21.

The histological data pertaining to the diameter of the blood vessels are graphically presented in Figures 6 and S4.

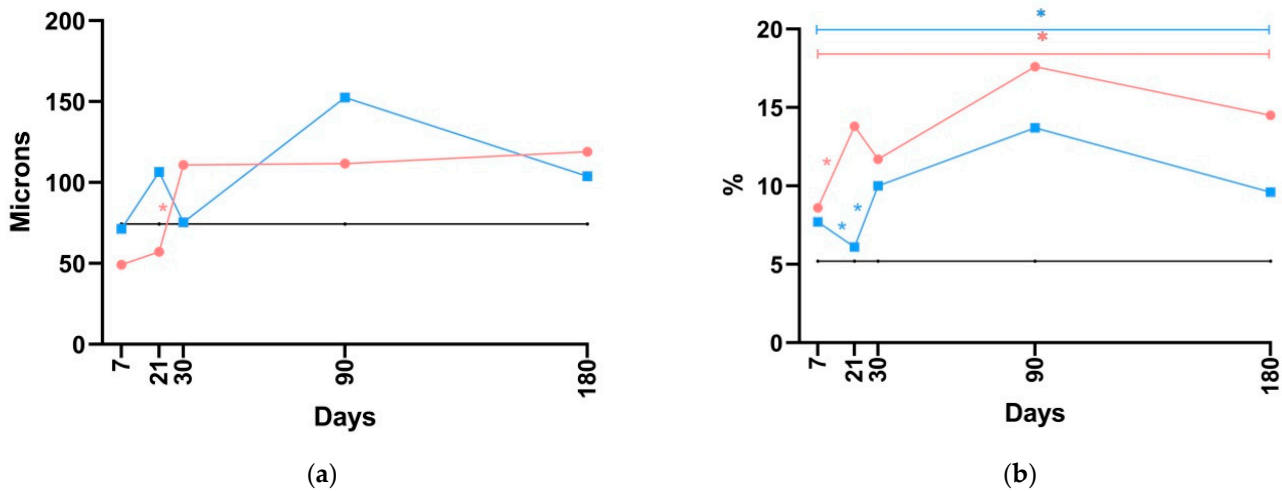


**Figure 6.** The linear graphs illustrate the changes in the diameter of blood vessels (a) and the relative vascular bed area (b) at five specific time points post-implantation, with median values used for graph construction. In these visuals, the *black* line represents the control group, whereas the *blue* and *red* lines correspond to P(LA/CL)-HA and P(LA/CL)-HA-micro threads, respectively. Data points that achieved a *p*-value of less than 0.05 were considered statistically significant, with an asterisk (\*) indicating those in the range of  $0.01 \leq p < 0.05$ .

#### 3.2.4. Relative Vascular Bed Area

*P(LA/CL)-HA-micro* vs. *Control*. During the entire period studied, the values for the relative vascular bed area were consistently greater with the use of P(LA/CL)-HA-micro than with the control. Statistically significant differences were observed on days 21, 90, and 180, whereas on day 30, there was a trend indicating the potential emergence of a statistically significant difference.

*P(LA/CL)-HA-micro* vs. *P(LA/CL)-HA*. For the relative vascular bed area, statistically significant differences when P(LA/CL)-HA and P(LA/CL)-HA-micro were used were observed only on day 21, with values for the P(LA/CL)-HA-micro threads significantly exceeding those of P(LA/CL)-HA. On other days, although the values for P(LA/CL)-HA-micro were greater than those for P(LA/CL)-HA, the differences were not statistically significant.

The outcomes of the histological analysis, which focused on measuring the diameter of blood vessels, are visually depicted in Figures 6 and S5.

#### 3.2.5. Fibrocytes

*P(LA/CL)-HA-micro* vs. *Control*. For the fibrocytes, the values obtained with P(LA/CL)-HA-micro were greater than the control values on days 7, 30, 90, and 180, with statistically significant differences observed on days 30 and 90 and a trend toward significance on day 180. On day 21, the values for P(LA/CL)-HA-micro were lower than those for the control, although the difference was not statistically significant.

*P(LA/CL)-HA-micro* vs. *P(LA/CL)-HA*. Statistically significant differences in the fibrocytes when P(LA/CL)-HA and P(LA/CL)-HA-micro were used were noted only on day 21, with values for P(LA/CL)-HA substantially exceeding those of P(LA/CL)-HA-micro. Interestingly, both thread types significantly increased in this parameter from day 21 to day 30, followed by a sharp decline by day 90, although there were no significant differences between P(LA/CL)-HA and P(LA/CL)-HA-micro during these days. On days 21, 30, and 90, the number of fibrocytes was greater with P(LA/CL)-HA-micro than with P(LA/CL)-HA, whereas on days 7 and 180, a slight advantage was observed with P(LA/CL)-HA over P(LA/CL)-HA-micro.

The histological data focusing on fibrocytes are shown in Figures 7 and S6.

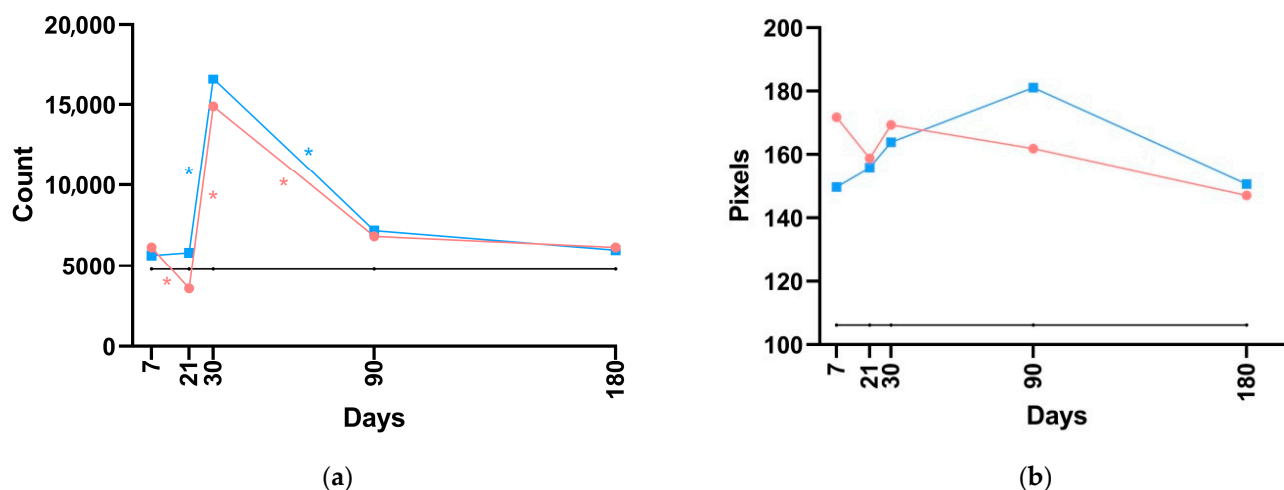


**Figure 7.** The linear graphs depict data concerning fibrocytes (a) and collagen density (b) at five separate time points during the post-implantation period, with median values used for each graph. In these charts, the control group is illustrated with a *black* line, P(LA/CL)-HA threads are indicated with a *blue* line, and P(LA/CL)-HA-micro threads are indicated with a *red* line. The results with a *p*-value of less than 0.05 were classified as statistically significant, with asterisks (\*) indicating values within the range of  $0.01 \leq p < 0.05$ .

### 3.2.6. Collagen Density

*P(LA/CL)-HA-micro* vs. *P(LA/CL)-HA*. The values for collagen density were greater when P(LA/CL)-HA-micro threads were used than when P(LA/CL)-HA was used, although the difference was not statistically significant.

The histological data pertaining to collagen density are graphically presented in Figures 7 and S7.

### 3.2.7. Density of Type I Collagen in the Dermis

*P(LA/CL)-HA-micro* vs. *Control*. The type I collagen in the dermis, when P(LA/CL)-HA-micro was used, exceeded the control level from days 21 to 90, with a statistically significant difference noted on day 30. On day 7, the levels of this parameter were lower than those in the control when P(LA/CL)-HA-micro was used, although the difference was not statistically significant. By day 180, the level of type I collagen significantly decreased when P(LA/CL)-HA-micro was used, which was significantly different from that of the control.

*P(LA/CL)-HA-micro* vs. *P(LA/CL)-HA*. The level of type I collagen in the dermis in the P(LA/CL)-HA group was significantly greater than that in the P(LA/CL)-HA-micro on days 7, 90, and 180. Conversely, on days 21 and 30, the levels were greater with P(LA/CL)-HA-micro than with P(LA/CL)-HA, although the differences were not statistically significant.

The histological data, which specifically target type I collagen in the dermis, are presented in Figures 8 and S8.

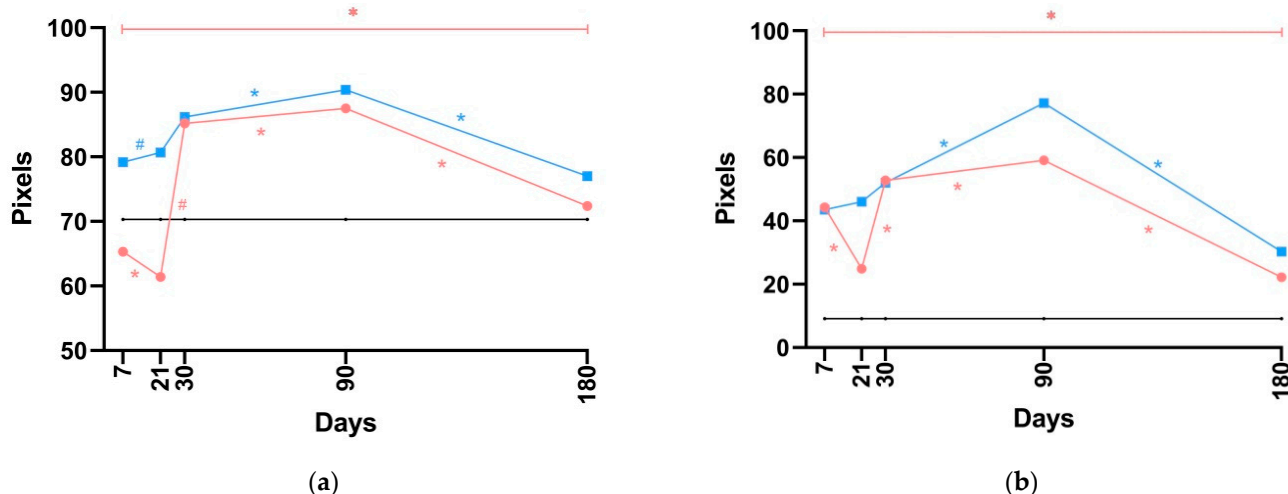


**Figure 8.** The linear graphs illustrate the changes in type I collagen density within the dermis (a) and hypodermis (b) at five distinct post-implantation intervals, constructed using median values. In these graphs, the black line represents the control group, whereas the blue and red lines represent the P(LA/CL)-HA and P(LA/CL)-HA-micro threads, respectively. Findings that yielded a  $p$ -value of less than 0.05 were deemed statistically significant, noted with an asterisk (\*) for values between 0.01 and 0.05. A hash symbol (#) denotes a trend towards significance for values between 0.05 and 0.1, suggesting potential significance with additional sampling.

### 3.2.8. Density of Type I Collagen in the Hypodermis

*P(LA/CL)-HA-micro vs. Control.* Throughout the duration of the study, the level of type I collagen in the hypodermis of P(LA/CL)-HA-micro consistently and significantly exceeded the control values.

*P(LA/CL)-HA-micro vs. P(LA/CL)-HA.* The level of type I collagen in the hypodermis, when P(LA/CL)-HA was used, was greater on days 21, 90, and 180 than the levels observed with P(LA/CL)-HA-micro, with the differences on days 21 and 90 being statistically significant. Conversely, on days 7 and 30, the effects of P(LA/CL)-HA-micro were not statistically significant but slightly exceeded those of P(LA/CL)-HA.

The histological data, specifically those concerning type I collagen in the hypodermis, are presented in Figures 8 and S9.

### 3.2.9. Density of Type III Collagen in the Dermis

*P(LA/CL)-HA-micro vs. Control.* The levels of type III collagen in the dermis, when P(LA/CL)-HA-micro threads were used, were lower than the control values on days 7 and 21, with a trend toward a statistically significant difference noted on day 21. By day 30, the values had further decreased below the control levels, and by day 90, this difference became statistically significant.

*P(LA/CL)-HA-micro vs. P(LA/CL)-HA.* The type III collagen in the dermis, when P(LA/CL)-HA-HA-micro was used, exceeded the levels observed with P(LA/CL)-HA-HA on days 7, 21, 30, and 180, with the differences being statistically significant on days 7, 21, and 180. However, on day 90, the levels of P(LA/CL)-HA-HA were significantly greater than those of P(LA/CL)-HA-HA-micro. Notably, when P(LA/CL)-HA-HA threads were used, this parameter decreased throughout the entire study period. With P(LA/CL)-HA-HA-micro, a decrease was observed from day 7 to day 90, followed by a sharp and significant increase by day 180.

The histological findings, which specifically focus on type III collagen in the dermis, are graphically represented in Figures 9 and S10.

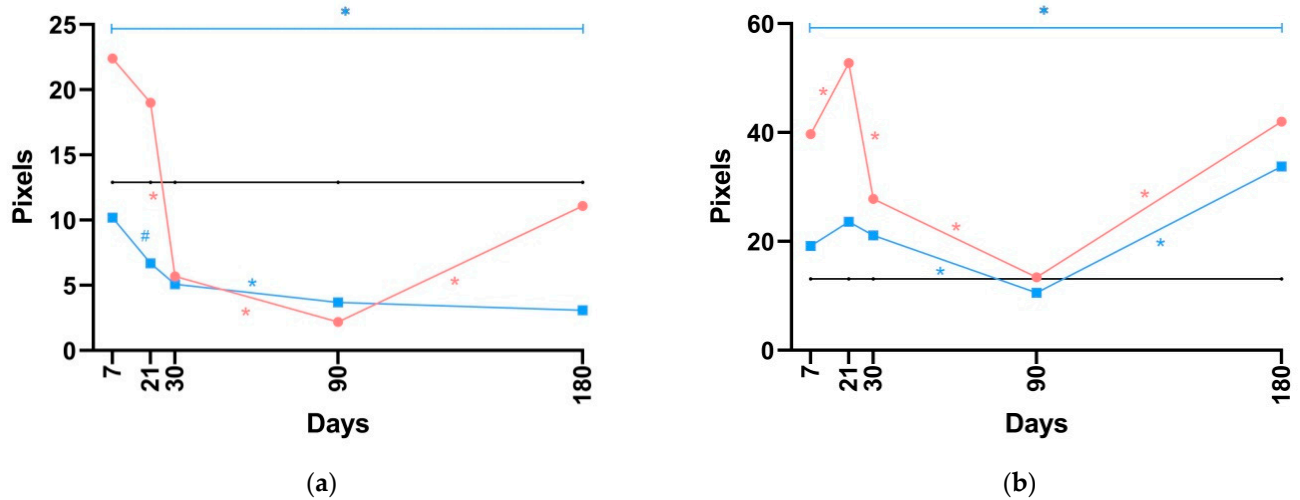


**Figure 9.** The linear graphs provide a systematic representation of the density of type III collagen in the dermis (a) and hypodermis (b) at five specific time points after implantation, with median values used for graph construction. In these visualizations, the control group is depicted by a black line, whereas the blue and red lines represent the P(LA/CL)-HA and P(LA/CL)-HA-micro threads, respectively. Outcomes that achieved a  $p$ -value of less than 0.05 were considered statistically significant, denoted with an asterisk (\*) for values between 0.01 and 0.05. A hash mark (#) indicates a  $p$ -value from 0.05 to 0.1, suggesting a potential trend toward significance, implying that conclusive results might be obtained with more extensive data collection.

### 3.2.10. Density of Type III Collagen in the Hypodermis

*P(LA/CL)-HA-micro vs. Control.* Throughout the study period, the levels of type III collagen in the hypodermis were consistently and significantly greater when P(LA/CL)-HA-micro was used, with the exception of day 90, when the values of this parameter were virtually equivalent to the control values.

*P(LA/CL)-HA-micro vs. P(LA/CL)-HA.* During the entire duration of the study, the level of type III collagen in the hypodermis in response to P(LA/CL)-HA-micro exceeded that in response to P(LA/CL)-HA, with statistically significant differences on days 7, 21, and 90. Notably, the levels peaked on day 21 when P(LA/CL)-HA-micro was used, followed by a decrease on days 30 and 90 and then an increase again on day 180. In the case of the P(LA/CL)-HA threads, there was also an increase by day 21, a decrease by days 30 and 90, and a subsequent increase on day 180, at which point the levels peaked.

The histological findings related to type III collagen in the hypodermis are visually depicted in Figures 9 and S11.

### 3.2.11. Ratio of Type I/III Collagen in the Dermis

*P(LA/CL)-HA-micro vs. Control.* The ratio of type I/III collagen in the hypodermis, when P(LA/CL)-HA-micro threads were used, was lower than the control values on days 7 and 21, with a trend toward a statistically significant difference observed on day 21. Conversely, on days 30, 90, and 180, the values of this parameter were greater than those of the controls when P(LA/CL)-HA-micro was used, with a statistically significant difference noted on day 90 and a trend toward significance noted on day 30.

*P(LA/CL)-HA-micro vs. P(LA/CL)-HA.* The ratio of type I/III collagen in the dermis, when P(LA/CL)-HA was used, exceeded the levels observed with P(LA/CL)-HA-micro on days 7, 21, 30, and 180, with statistically significant differences noted on days 7, 21, and 180. Conversely, on day 90, the values of this parameter were significantly greater when P(LA/CL)-HA-micro threads were used. Notably, with P(LA/CL)-HA, there was an increase in this parameter throughout the entire study period. In contrast, with P(LA/CL)-

HA-micro, the ratio increased from day 7 to day 90 but then sharply decreased to control values by day 180.

The histological data, specifically the ratio of type I to type III collagen in the dermis, are graphically presented in Figures 10 and S12.

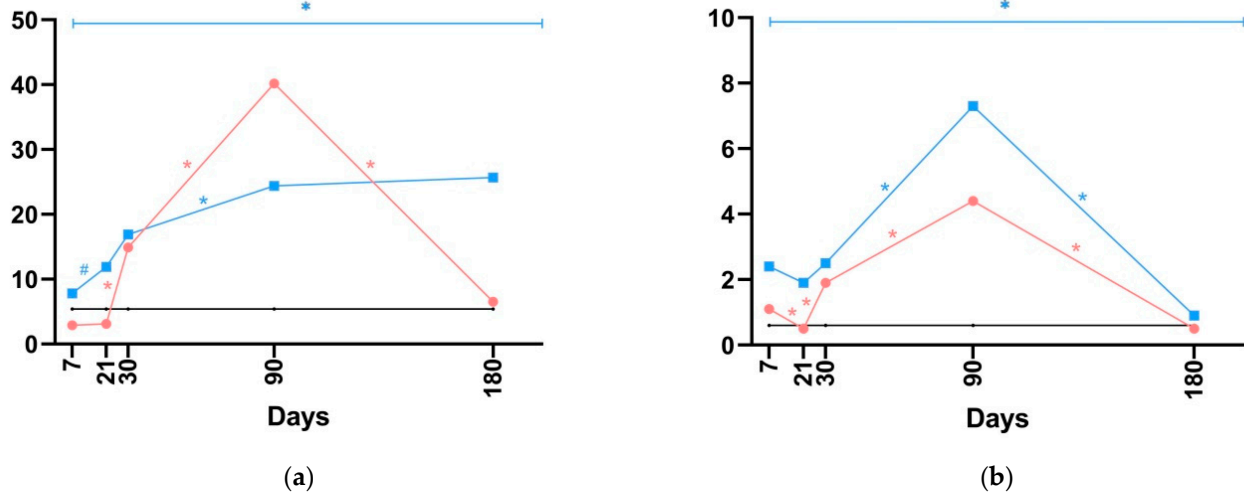


**Figure 10.** The linear graphs display data on the ratio of type I to type III collagen in the dermis (a) and hypodermis (b) at five distinct post-implantation intervals, constructed from median values. In these graphs, the control group is represented by a black line, whereas the blue and red lines represent the P(LA/CL)-HA and P(LA/CL)-HA-micro threads, respectively. Findings with a *p*-value less than 0.05 were classified as statistically significant, as noted with an asterisk (\*) for values between 0.01 and 0.05. A hash symbol (#) marks *p*-values between 0.05 and 0.1, indicating a trend toward significance, suggesting that definitive significance might be attainable with a larger dataset.

### 3.2.12. Ratio of Type I/III Collagen in the Hypodermis

*P(LA/CL)-HA-micro vs. Control.* The ratio of type I/III collagen in the hypodermis, when P(LA/CL)-HA-HA-micro threads were used, exceeded the control values on days 7, 30, and 90, with these differences being statistically significant. On days 21 and 180, this parameter was slightly lower than that of the control when P(LA/CL)-HA-HA-micro was used, although the differences were not statistically significant.

*P(LA/CL)-HA-micro vs. P(LA/CL)-HA.* During the entire duration of the study, the ratio of type I/III collagen in the hypodermis when P(LA/CL)-HA was used consistently exceeded the values observed with P(LA/CL)-HA-micro, with statistically significant differences noted on days 7, 21, and 90. Importantly, for both thread types, there was a decrease in the values of this parameter between days 7 and 21, followed by a slight increase by day 30 and a sharp increase by day 90. By day 180, this parameter had decreased for both P(LA/CL)-HA and P(LA/CL)-HA-micro.

The histological findings focused on the ratio of type I to type III collagen in the hypodermis are visually displayed in Figures 10 and S13.

### 3.2.13. Density of Elastin in the Dermis

*P(LA/CL)-HA-micro vs. Control.* During the entire study period, elastin levels in the dermis when P(LA/CL)-HA-micro threads were used were consistently greater than the control values. Statistically significant differences were observed on days 30, 90, and 180, with a trend towards significant differences noted on day 21.

*P(LA/CL)-HA-micro vs. P(LA/CL)-HA.* Throughout the study period, no statistically significant differences were observed in elastin levels in the dermis. Notably, with the use of P(LA/CL)-HA-micro threads, there was a consistent increase in values across all days.



For P(LA/CL)-HA, an increase was also observed from day 7 to day 30; however, the levels decreased by day 90 and increased again by day 180.

The histological results, which specifically analyze elastin in the dermis, are visually presented in Figures 11 and S14.

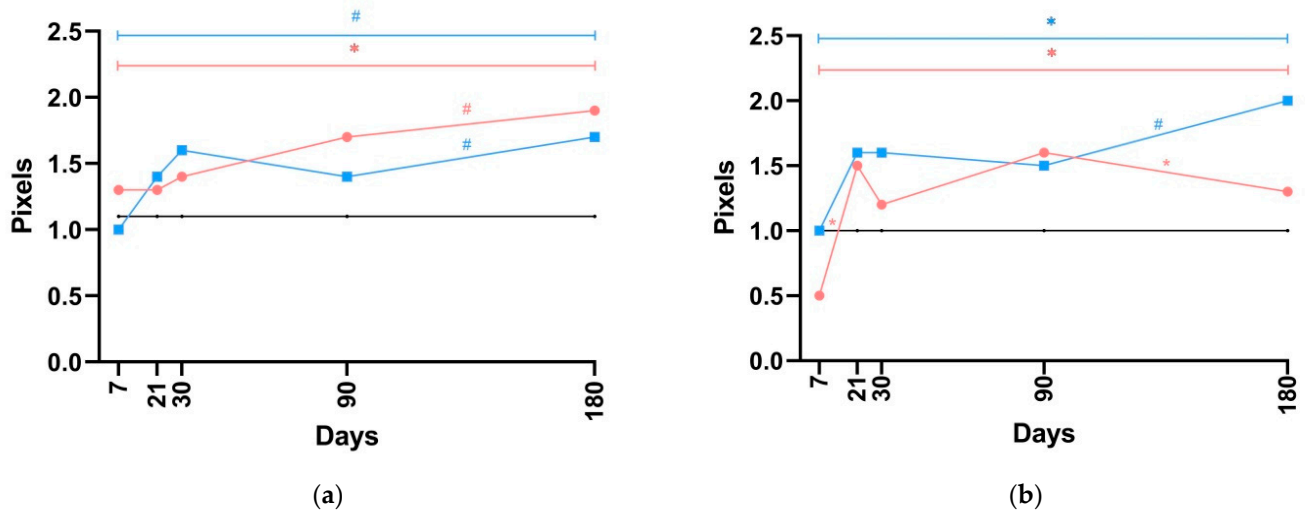


**Figure 11.** The linear graphs present data on elastin density in the dermis (a) and hypodermis (b) across five distinct time points after implantation, with median values used for construction. These graphs depict the control group with a black line, while the P(LA/CL)-HA threads are shown in blue, and the P(LA/CL)-HA-micro threads are shown in red. The results with a  $p$ -value less than 0.05 were deemed statistically significant and are marked with an asterisk (\*) for values between 0.01 and 0.05. A hash symbol (#) indicates  $p$ -values between 0.05 and 0.1, indicating a trend towards significance and suggesting that conclusive results could be obtained with a larger dataset.

#### 3.2.14. Density of Elastin in the Hypodermis

*P(LA/CL)-HA-micro vs. Control.* On day 7, the levels of elastin in the hypodermis when P(LA/CL)-HA-micro threads were used were lower than those of the control, although the difference was not statistically significant. By day 21, this parameter had increased, with levels exceeding those of the control. Statistically significant differences were observed on days 21 and 180, and there was a trend toward significant differences on day 90.

*P(LA/CL)-HA-micro vs. P(LA/CL)-HA.* No statistically significant differences were observed in the levels of elastin in the hypodermis across most time intervals, except for day 21, when a trend towards a significant difference was noted. On days 21, 90, and 180, the levels when P(LA/CL)-HA-micro was used were greater than those when P(LA/CL)-HA was used. Conversely, on day 7, the levels were slightly greater with P(LA/CL)-HA than with P(LA/CL)-HA-micro. By day 30, the levels for both thread types were nearly identical.

The histological findings, which specifically address elastin levels in the hypodermis, are visually detailed in Figures 11 and S15.

## 4. Discussion

### 4.1. Dermal Thickness

In our study, the dynamic changes in dermal thickness over the six-month period provide insightful data into the behavior of P(LA/CL)-HA-micro threads in comparison to the control and P(LA/CL)-HA threads. The dermal thickness of the region threaded by P(LA/CL)-HA-micro threads tended to be consistently lower than that of the control from day 7 through day 90, with significant differences during this period ( $p = 0.0431$  on days 7, 21, and 30). Interestingly, by day 180, there was a marked increase in dermal thickness in the P(LA/CL)-HA-micro group, which significantly surpassed the control

levels ( $p = 0.0431$ ). This late-stage surge in dermal thickness could be indicative of a delayed but robust remodeling response, likely facilitated by the sustained release of hyaluronic acid, which may have contributed to prolonged tissue remodeling and rejuvenation.

When P(LA/CL)-HA-micro threads were directly compared with P(LA/CL)-HA threads, the P(LA/CL)-HA threads consistently presented greater dermal thickness across most of the study period, with significant differences observed on days 21, 30, and 90 ( $p = 0.0431$  for each). These differences point to a more immediate and consistent effect on dermal thickening caused by the P(LA/CL)-HA threads than by their microencapsulated counterparts. By day 180, however, the gap between the two thread types narrowed, with a trend indicating that P(LA/CL)-HA-micro threads may capture the effects of P(LA/CL)-HA threads in terms of dermal thickness ( $p = 0.0796$ ).

This observed pattern in our study involving a pig model indicates that P(LA/CL)-HA-micro threads demonstrate a statistically significant, albeit delayed, increase in dermal thickness compared with the control. This finding suggests the potential for improved long-term aesthetic outcomes in similar scenarios requiring sustained tissue support and gradual rejuvenation. While P(LA/CL)-HA threads were more immediate and expressed increases in dermal thickness, the kinetics of HA release from the microencapsulated threads were still favorable for gradual tissue remodeling within the context of our animal model.

Importantly, while these findings are promising and suggest a pattern that might reduce the risk of overtreatment—a common concern in thread lifting—these findings are derived from a pig model. Thus, the initial lower thickness observed with P(LA/CL)-HA-micro threads and the eventual increase in dermal thickness that could lead to more durable and natural-looking skin rejuvenation must be interpreted with caution.

#### 4.2. Thickness of the Fibrous Sheath

The thickness of the fibrous sheath is a critical indicator of the fibrotic response following thread implantation, reflecting the biocompatibility and biofunctionality of the thread materials in tissue integration and remodeling.

Our findings illustrate an increase in the thickness of the fibrous sheath around both types of threads at multiple intervals, highlighting the dynamic tissue responses induced by the thread implants.

In the case of P(LA/CL)-HA-micro threads, which feature microencapsulated HA designed for sustained release, significant decreases in thickness were observed from day 7 to day 21, followed by a subsequent increase from day 21 to day 30 ( $p = 0.0431$ ). From day 30 to day 90, no significant change was observed ( $p = 0.6858$ ). However, a gradual and significant decrease was observed from day 90 to day 180, as well as from day 7 to day 180 ( $p = 0.0431$ ), indicating a reduction in the expression of the long-term fibrotic response. This reduction could be attributed to the controlled release of HA, potentially influenced by the persistent anti-inflammatory properties associated with continuous release.

When the two thread types were compared directly, P(LA/CL)-HA-micro threads initially exhibited a significantly greater fibrous sheath thickness on day 7 than did P(LA/CL)-HA ( $p = 0.0431$ ). However, subsequent intervals showed the opposite trend, with P(LA/CL)-HA threads demonstrating greater fibrous sheath thickness, where statistically significant differences were observed on days 21, 30, and 180 ( $p = 0.0431$ ). These significant differences can be attributed to the differing kinetics of hyaluronic acid bioavailability. On day 7, the P(LA/CL)-HA threads, benefiting from a greater initial increase in hyaluronic acid, suppressed the inflammatory response more effectively. In contrast, the P(LA/CL)-HA-micro threads did not achieve the necessary hyaluronic acid levels initially. Over time, the lack of controlled-release technology in P(LA/CL)-HA threads led to more pronounced thickening of the capsule-like structures due to hyaluronic acid depletion. Conversely, in

P(LA/CL)-HA-micro threads, the fibrous response is moderated in a smoother manner, thereby avoiding a more pronounced oscillatory pattern.

Our findings indicate that P(LA/CL)-HA-micro threads demonstrate a more moderate fibrous sheath response over time. This is evident from the significant decreases in fibrous sheath thickness at various intervals, suggesting the potential for improved long-term biocompatibility and reduced fibrosis compared with P(LA/CL)-HA threads. From a clinical perspective, especially in a veterinary setting, these results suggest that P(LA/CL)-HA-micro threads could offer more favourable outcomes in terms of tissue integration and healing.

The reduced fibrosis and moderate fibrous response observed in the P(LA/CL)-HA-micro threads could translate to less scarring and potentially enhanced aesthetic outcomes in clinical applications, but clinical trials are needed.

#### 4.3. Morphometric Characteristics of Vasculature

We explored the impact of P(LA/CL)-HA-micro threads on the diameter of blood vessels and the relative vascular bed area in the skin surrounding the lifting threads, which can indicate not only vascular responses related to tissue perfusion but also broader tissue health and regeneration capabilities prompted by the thread implants.

P(LA/CL)-HA-micro threads exhibited a dynamic vascular response, with vessel diameters initially below control values on days 7 and 21, probably indicating neoangiogenesis. A significant increase occurred by day 30 ( $p = 0.0431$ ), suggesting a robust angiogenic response, which likely modulates long-term vascular adaptation.

Despite differences in dynamic patterns, a trend toward statistical significance was observed on day 90 for P(LA/CL)-HA threads and on day 180 for both types of threads ( $p = 0.0796$ ) compared with the control.

Changes in the relative vascular bed area significantly increased from days 7 to 21 ( $p = 0.0431$ ), with stabilization thereafter. However, cumulative analysis from days 7 to 180 indicated a sustained overall increase ( $p = 0.0431$ ), surpassing P(LA/CL)-HA threads ( $p = 0.0094$ ). This delayed yet enhanced vascularization likely results from prolonged release of bioactive agents by microencapsulation technology, supporting improved tissue perfusion.

Compared with the control, P(LA/CL)-HA-micro threads demonstrated statistically significant differences on days 21, 90, and 180, and a trend toward statistically significant changes was detected on day 30. This finding indicates pronounced vascular changes throughout nearly the entire observation period ( $p = 0.0000$ ).

P(LA/CL)-HA threads resulted in larger vessel diameters on days 7, 21, and 90, whereas P(LA/CL)-HA-micro threads resulted in greater increases on days 30 and 180. However, a trend toward significance was noted only on day 21 ( $p = 0.0796$ ). On other days, no significant differences were noted.

In terms of the relative vascular bed area, direct comparisons revealed that on day 21, P(LA/CL)-HA-micro threads significantly outperformed P(LA/CL)-HA threads ( $p = 0.0431$ ). While other time points did not reach statistical significance, a consistent trend favoring P(LA/CL)-HA-micro threads was evident throughout the study.

In a porcine model, we observed that P(LA/CL)-HA-micro threads enhance the vascular response and tissue perfusion over time. This enhancement is predominantly evident through changes in the relative vascular bed area, rather than alterations in vessel diameter, compared with both the control group and the P(LA/CL)-HA threads. Enhanced vascularization is critical for improving tissue viability and health following surgical interventions. In clinical practice, this could translate to better wound healing processes, a reduced risk of complications, and improved aesthetic outcomes for patients undergoing reconstructive or cosmetic procedures involving thread lifts.

#### 4.4. Fibrocytes

In general, the dynamic patterns for both types of threads were quite similar, peaking on the 30th day and subsequently decreasing from the 90th day to the 180th day, except for a statistically significant difference on the 21st day ( $p = 0.0431$ ). On day 21, the dynamics of the fibrocyte response between the P(LA/CL)-HA-micro and P(LA/CL)-HA threads highlighted their distinct interactions with the biological environment. The P(LA/CL)-HA threads presented a significant increase in fibrocyte activity, indicative of a rapid fibrotic response due to the unrestricted availability of HA, which stimulates fibroblast proliferation [20]. In contrast, the P(LA/CL)-HA-micro threads, featuring microencapsulated HA for controlled release, exhibited a moderate decrease in fibrocyte counts, suggesting delayed activation that aligns more closely with inherent tissue remodeling.

The observed interactions of P(LA/CL)-HA and P(LA/CL)-HA-micro threads within our animal model indicate divergent mechanisms of tissue integration and remodeling. The P(LA/CL)-HA threads prompt an accelerated fibrotic response attributable to their unimpeded availability of hyaluronic acid. This enhanced fibrocyte activity may prove advantageous for applications necessitating immediate stabilization of the implant, potentially augmenting dermal stability and diminishing the timeframe required to attain aesthetic outcomes.

Conversely, P(LA/CL)-HA-micro threads exhibit delayed but sustained fibrocyte activity that minimizes early inflammation. This pattern suggests a remodeling process that more closely mimics gradual tissue healing, potentially reducing the risk of complications such as scarring and fibrotic encapsulation, which can be beneficial in enhancing long-term aesthetic outcomes in the case of projection onto a human being.

#### 4.5. Collagenogenesis

The primary collagens found in the extracellular matrix (ECM) are types I and III [21]. In the skin, type I collagen makes up 80–85% of the dermal ECM, whereas type III collagen accounts for approximately 8–11% [22]. Type I collagen is a rigid, fibrillar protein that provides tensile strength, whereas type III collagen forms an elastic network [21].

In the case of P(LA/CL)-HA-micro threads, a trend towards a significant increase in collagen density was demonstrated in the dermis from day 21 to day 30 post-implantation ( $p = 0.0796$ ), reaching levels comparable to those observed with P(LA/CL)-HA threads, albeit after an initial decrease. The type I collagen density values on days 7 and 21, although lower than those in the control, were not statistically significant, suggesting a gradual initiation of the collagenogenic response that becomes more pronounced and effective over time. The same pattern was observed in the hypodermis, but with a statistically significant increase from day 21 to day 30 ( $p = 0.0431$ ). Compared with those in the control, significant increases in the hypodermis were consistently observed from day 7 to day 180, with  $p$ -values reaching 0.0431, whereas in the dermis, substantial differences were noted only on days 30 and 180 ( $p = 0.0431$ ).

The statistical data underscore the predominant efficacy of both types of threads in maintaining elevated collagen levels, surpassing those of the controls at almost every measured point, thereby indicating their improved performance in promoting and maintaining collagen density, specifically in the hypodermis.

On the other hand, only the P(LA/CL)-HA-micro threads significantly increased type I collagen production in both the dermis and the hypodermis from days 7 to 180 ( $p = 0.0431$ ).

Direct comparisons between P(LA/CL)-HA-micro and P(LA/CL)-HA threads revealed nuanced differences in their influence on collagen density. In both the dermis and hypodermis, the densities of type I collagen were similar on day 30 and significantly different by day 90 ( $p = 0.0431$ ). Generally, the dynamic patterns were similar to each other,

except for the initial point where on day 7, values in the hypodermis were akin, but in the dermis, they were significantly different, with P(LA/CL)-HA threads surpassing those of P(LA/CL)-HA-micro threads.

Finally, in the pig model, we observed that P(LA/CL)-HA threads consistently presented higher levels of type I collagen than P(LA/CL)-HA-micro threads did, which is indicative of a robust and sustained collagen response. These differences likely stem from the variations in the availability of hyaluronic acid within the thread compositions. Specifically, the encapsulated form of hyaluronic acid in the P(LA/CL)-HA-micro threads allows for more controlled and gradual release, leading to less pronounced stimulation of type I collagenogenesis, suggesting a low-stimulating effect. While these results provide valuable insights into the potential mechanisms driving collagen production, their translation to clinical relevance requires careful consideration.

A significant parabola-like pattern in type III collagen production was noted during the treatment period in the dermis, with peak initial values on day 7 and much lower values on day 180, without a significant difference between these two time points ( $p = 0.2249$ ). This finding indicates a robust initial response to the threads, reflecting their effectiveness in stimulating early collagen synthesis, followed by a resurgence to minimum values by day 90. A similar but slightly different, statistically significant wave-like pattern in the initial period is distinguished in the hypoderm. Notably, the data revealed a peak in collagen density on day 21 ( $p = 0.0431$ ), followed by a stabilization period where the density almost aligned with control values on day 90 ( $p = 0.8927$ ) and a subsequent resurgence by day 180 ( $p = 0.0431$ ). This fluctuation suggests a dynamic remodeling process influenced by the sustained release of hyaluronic acid from the threads.

In comparison, the density of type III collagen in the dermis was greater than that of the control in the initial phase (day 7, with a trend toward significance on day 21 ( $p = 0.0796$ )), suggesting that the threads might temporarily facilitate new matrix structurization. However, by day 90 ( $p = 0.0431$ ), a significant decrease relative to the control suggested that the initial suppression led to new matrix deposition, which became less pronounced by the end of the experiment (there was no significant difference between the control and P(LA/CL)-HA-micro threads' values on day 180 ( $p = 0.8401$ )). In the case of the hypodermis, compared with the dermis, P(LA/CL)-HA-micro threads consistently facilitated higher levels of type III collagen, with significant differences noted on all study days except day 90, illustrating the continuous impact of the threads on the hypodermal collagen framework through general stimulation of type III collagen synthesis.

Throughout the study, P(LA/CL)-HA-micro threads consistently showed an increased capacity to modulate type III collagen density in the dermis compared with P(LA/CL)-HA, with significantly greater levels in both the initial and final phases (days 7, 21, and 180) ( $p = 0.0431$ ). This enhancement may be attributable to the continuous release of HA, which potentially provides a more sustained stimulus for collagen synthesis.

In the case of the hypodermis, P(LA/CL)-HA-micro threads demonstrated improved performance in enhancing type III collagen density throughout the study period. Significantly higher collagen levels were observed on days 7, 21, and 90 ( $p = 0.0431$  for each), indicating a more pronounced and sustained effect of the microencapsulated HA in these threads. However, by the end of the experiment, no statistically significant differences were identified between the treatments.

Our results conclusively indicate that both types of threads substantially affect type III collagen density, with P(LA/CL)-HA-micro threads demonstrating especially pronounced activity within both the dermis and hypodermis layers. The observed patterns of type III collagen density, reminiscent of parabola-like and wave-like formations, suggest intricate interactions between the implanted materials and the host tissue. These interactions are

characterized by an initial surge in collagen production on days 7 and 21, followed by a subsequent reduction or return to baseline levels. This dynamic pattern may reflect the threads' capacity to initially reinforce the structural integrity of porcine skin, which could theoretically translate to increased skin firmness in humans.

The early increase in collagen production may also play a critical role in augmenting the initial stages of wound healing by providing a scaffold conducive to new tissue formation. Additionally, the sustained release of hyaluronic acid from the P(LA/CL)-HA-micro threads seems to foster a prolonged collagenogenic response, notably in the hypodermis. Although these findings are encouraging, the application of these results from porcine models to human clinical treatments requires cautious consideration.

Adjustment of the ECM composition, especially the proportional relationship between type I and type III collagen, is crucial in the field of aesthetic medicine. The quantitative ratio of type I to type III collagen is a significant indicator of ECM maturation and the integrity of tissue remodeling subsequent to the implantation of bioabsorbable threads [21].

Significant changes in the ratio of type I to III collagen in the dermis were noted for P(LA/CL)-HA-micro threads, particularly from day 21 to day 90 ( $p = 0.0431$  at each interval), indicating a substantial modification in the collagen composition. This shift suggests an active remodeling phase in which the quality and type of collagen are altered by the presence of threads. A similar pattern was observed in the hypodermis, with significant alterations and a peak on day 90 ( $p = 0.0431$ ), indicating a potent effect of the threads on modulating collagen types within the hypodermis. These changes indicate the role of threads in enhancing or possibly accelerating the maturation process from type III collagen (often associated with early wound healing) to type I collagen (associated with mature, structurally sound tissue).

Initially, in the dermis, the ratio of P(LA/CL)-HA-micro threads was lower than that of the control on days 7 and 21 ( $p = 0.3452$  and  $0.0796$ , respectively) because of the potential degradation of some of the existing collagen framework to lay down new matrix material. However, in both the dermis and hypodermis, the final values reached levels comparable to the control values by day 180 ( $p = 0.6858$ ).

At the beginning, the lower ratio of type I/III collagen could be attributed to the increased deposition of type III collagen, a marker of early wound healing. Over time, as type I collagen synthesis commenced and matured, there was a notable increase in the ratio, indicating a progression toward more robust and structurally stable collagen that characterizes long-term tissue repair and remodeling.

A comparison of thread types revealed that P(LA/CL)-HA-micro threads promoted a pronounced collagen ratio after day 30, reflecting their statistically significant mid-term engagement ( $p = 0.0431$  on day 90) with the healing process and tissue remodeling. Conversely, in the hypodermis, both threads reached comparable values at the time of the last time point, whereas in the dermis, the P(LA/CL)-HA values significantly exceeded those of P(LA/CL)-HA-micro. This finding indicates the formation of a more mature collagen network in the long term with P(LA/CL)-HA.

Our research revealed substantial alterations in the ratio of type I to type III collagen subsequent to the implantation of P(LA/CL)-HA-micro threads. The marked efficacy of these threads in both the dermal and hypodermal layers signifies a vigorous phase of tissue remodeling. These modifications could have implications for clinical applications, potentially yielding benefits such as improved aesthetic results and hastened recovery following interventions, facilitated by the accelerated maturation of collagen. Notably, the transition from type III to type I collagen, which is associated with more mature and structurally robust tissue, may decrease the likelihood of complications such as scarring and enhance the overall structural integrity of the skin.



Moreover, the initial surge in type III collagen, typically associated with the early phases of wound healing, followed by a marked elevation in type I collagen, underscores a dynamic and favourable remodeling process. This aspect is especially beneficial in clinical scenarios aimed at reinforcing the skin structure and diminishing the visible effects of aging or damage. These findings suggest that these threads could be instrumental in advancing dermatological health and cosmetic outcomes.

However, these results were obtained from an animal model. While porcine skin closely resembles human skin in terms of structure and function, the direct translation of these results to human patients requires cautious interpretation.

#### 4.6. Elastogenesis

For P(LA/CL)-HA-micro threads, initial observations in the dermis revealed no significant changes in elastin levels from day 7 to day 90 ( $p > 0.05$ ), suggesting a latent phase before any notable biochemical activity becomes apparent. However, a gradual increase became notable from day 30 onwards, maintaining this significance through days 90 and 180, with a trend toward significance at the last time point ( $p = 0.0431$ ). This increase signifies the role of the threads in enhancing elastin synthesis or stabilization, possibly influenced by the sustained release properties of HA microencapsulation. In the hypodermis, a different pattern was observed, which can be characterized as wave-like. The analysis revealed a statistically significant increase in the density of elastin by day 21 ( $p = 0.0431$ ), peaking on day 90, with a subsequent decrease until the last time point ( $p = 0.0431$ ). This suggests an initial increase in elastin synthesis or restructuring, followed by sustained enhancement, likely due to the continuous influence of the microencapsulated HA.

Notably, only the P(LA/CL)-HA-micro threads significantly affected the stimulation of elastogenesis from days 7 to 180 in both the dermis and hypodermis ( $p = 0.0431$ ).

Compared with the control values, the elastin density in response to P(LA/CL)-HA-micro threads tended to increase consistently, with significant increases notably beginning on day 21 ( $p = 0.0796$ ) and extending throughout the study period. This finding indicates a robust influence of the threads on the dermal matrix, supporting the development of a more elastic and durable tissue structure. In the case of the hypodermis, the initial decrease observed on day 7 ( $p = 0.1380$ ), when the levels were below those of the control, may reflect a transient adjustment or redistribution phase within the hypodermal tissues in response to thread implantation. Over the entire duration of the study, the elastin levels in the P(LA/CL)-HA-micro threads were consistently greater than those in the control from day 21 onwards. A significant difference was noted only on days 21 and 180 ( $p = 0.0431$ ), but there was also a trend toward significance on day 90 ( $p = 0.0796$ ).

In light of the marked enhancement in elastin synthesis observed within both the dermal and hypodermal layers of our porcine model, the deployment of P(LA/CL)-HA-micro threads has considerable potential for translational clinical benefits. Owing to their dermatological congruence with humans, the present study leveraged pigs and documented a substantial elevation in elastin concentrations, the implications of which may extend to augmented tissue resilience and elasticity within a clinical milieu. Such attributes are paramount for applications within the realm of aesthetic medicine, wherein augmented elastin production could culminate in improved cosmetic outcomes and a decrease in procedural complications, including scarring and loss of tissue elasticity.

While our findings reveal that both thread variants facilitate an increase in elastin without statistically significant disparities in efficacy ( $p > 0.05$ ), the observed patterns of elastin dynamics—characterized by progressive increases in the dermis and oscillatory modifications in the hypodermis—point to divergent mechanistic pathways or differential responses to the HA encapsulated within the threads. This suggests a nuanced interplay of

the threads with the surrounding tissue matrix, meriting further investigation into their respective mechanisms of action.

Furthermore, the sustained increase in elastin density observed from day 21 onwards, especially when contrasted with the control values, substantiated the formation of a more robust dermal matrix. This enhancement could prove particularly advantageous in clinical contexts where tissue integrity and elasticity are diminished.

## 5. Conclusions

The histological analysis of P(LA/CL)-HA-micro threads in a pig model underscores their role in fostering enhanced and sustainable skin remodeling outcomes. These threads, equipped with a microencapsulated HA delivery system (NAMICA technology) (APTOS LLC (Tbilisi, Georgia)), facilitate a delayed yet robust increase in dermal thickness, resulting in more physiologically favorable outcomes in an animal model. The kinetic disparity in HA release from our model suggests the potential for improved long-term aesthetic outcomes that may align closely with natural tissue remodeling processes, although verification in human models is needed.

Furthermore, the controlled release of HA from the microencapsulated threads moderates fibrous sheath responses, indicating reduced fibrosis and enhanced biocompatibility over extended periods in pigs. These findings suggest that P(LA/CL)-HA-micro threads could enhance the vascular response and tissue perfusion, primarily through alterations in the relative vascular bed area rather than mere changes in vessel diameter, thus promoting healthier tissue integration from day 30 to day 180 post-implantation.

Moreover, the subtle yet statistically significant stimulation of type I collagen synthesis, alongside the dynamic modulation of type III collagen, highlights the ability of threads to shift the ECM composition from one predominantly featuring type III collagen (indicative of early wound healing) to a more mature structure enriched with type I collagen, mostly by the 90th day. This transition, which is crucial for long-term tissue integrity in an animal model, may offer insights into accelerating ECM maturation in human applications.

Finally, the significant increase in elastin synthesis in both the dermis and hypodermis of pigs contributes to a more elastic and durable tissue structure over time, underscoring the sophisticated approach of P(LA/CL)-HA-micro threads in aligning skin remodeling with the smooth healing dynamics observed in our animal model.

In conclusion, while P(LA/CL)-HA-micro threads represent promising advancements in bioabsorbable thread technology for aesthetic medicine, their clinical benefits in humans remain to be established through rigorous clinical trials. Future investigations should strive to reconcile these encouraging preclinical findings with tangible patient advantages, emphasizing the direct effects that such structural improvements may have on clinical outcomes, including diminished recovery durations and increased long-term incorporation and function of implanted materials.

**Supplementary Materials:** The following supporting information can be downloaded at <https://www.mdpi.com/article/10.3390/cosmetics12010020/s1>, Figure S1: The collection comprises a series of macroscopic photographs illustrating specimens of skin and subcutaneous tissue, excised from a 15 cm segment of harvested soft tissue at two distinct time points. Figure S2: A series of box plots presents measurements of dermal thickness for three distinct groups—the control, P(LA/CL)-HA-micro, and P(LA/CL)-HA—at five different time points in the post-implantation period. Figure S3: A collection of box plots graphically represents measurements of fibrous sheath thickness among two groups—P(LA/CL)-HA-micro and P(LA/CL)-HA—over five distinct time points in the post-implantation phase. Figure S4: A collection of box plots graphically illustrates the diameter of blood vessels across three groups—the control, P(LA/CL)-HA-micro, and P(LA/CL)-HA—at five points during the post-implantation period. Figure S5: A series of box plots graphically

displays data on the relative vascular bed area among three groups—the control, P(LA/CL)-HA-micro, and P(LA/CL)-HA—over five distinct time intervals following implantation. Figure S6: A sequence of box plots visually presents data on fibrocyte counts among three different groups—the control, P(LA/CL)-HA-micro, and P(LA/CL)-HA—at five distinct time intervals following implantation. Figure S7: A series of box plots systematically presents data on collagen density for two specific groups, P(LA/CL)-HA-micro and P(LA/CL)-HA, at five distinct post-implantation time points. Figure S8: A collection of box plots systematically displays data on the density of type I collagen in the dermis across three groups: the control, P(LA/CL)-HA-micro, and P(LA/CL)-HA, over five specific time points in the post-implantation phase. Figure S9: A sequence of box plots effectively illustrates the density of type I collagen in the hypodermis for three distinct groups: the control, P(LA/CL)-HA-micro, and P(LA/CL)-HA, at five designated time points following implantation. Figure S10: A set of box plots methodically presents the density of type III collagen in the dermis across three groups: the control, P(LA/CL)-HA-micro, and P(LA/CL)-HA, at five consecutive time points following implantation. Figure S11: A series of box plots meticulously presents the density of type III collagen in the hypodermis for three groups: the control, P(LA/CL)-HA-micro, and P(LA/CL)-HA, measured at five specific time points during the post-implantation phase. Figure S12: A series of box plots methodically captures data on the ratio of type I to type III collagen in the dermis across three specific groups: the control, P(LA/CL)-HA-micro, and P(LA/CL)-HA, at five different time points during the post-implantation phase. Figure S13: A collection of box plots was created to depict the ratios of type I to type III collagen in the hypodermis among three groups: the control, P(LA/CL)-HA-micro, and P(LA/CL)-HA, observed at five distinct time points during the post-implantation phase. Figure S14: A sequence of box plots systematically visualizes data on the density of elastin in the dermis for three distinct groups: the control, P(LA/CL)-HA-micro, and P(LA/CL)-HA, over five consecutive time points in the post-implantation phase. Figure S15: A series of box plots methodically displays the density of elastin in the hypodermis for three distinct groups—the control, P(LA/CL)-HA-micro, and P(LA/CL)-HA—across five specific time points during the post-implantation phase. Table S1: Descriptive statistics for P(LA/CL)-HA on each studied day and across all days combined. Table S2: Descriptive statistics for P(LA/CL)-HA-micro on each studied day and across all days combined. Table S3: Descriptive statistics for the control samples on each studied day and across all days combined

**Author Contributions:** Conceptualization, P.B., G.S. and D.N.; methodology, P.B. and D.N.; software, P.B.; validation, D.N.; formal analysis, P.B.; investigation, P.B. and D.N.; resources, G.S.; data curation, P.B.; writing—original draft preparation, P.B.; writing—review and editing, D.N.; visualization, P.B.; supervision, D.N.; project administration, P.B.; funding acquisition, G.S. All authors have read and agreed to the published version of the manuscript.

**Funding:** The logistical needs of P.B. were supported by the institutional doctoral fund PJ\_DR\_D24\_INCR10\_37\_523976\_BURKO from the University of Palermo (Palermo, Italy). Additionally, this research received funding from APTOS LLC (Tbilisi, Georgia) under grant number No. 21/08/2023-3. The article processing charges (APC) were privately covered by P.B.

**Institutional Review Board Statement:** This study was carried out following the guidelines sanctioned by the Local Ethics Committee (LEC) of the LLC “Preclinical Research Center” (Penza, Russia). The research protocol was officially authorized by the LEC under protocol number 5-2023, dated 23 August 2023. This experimental animal study complies with ethical norms and international requirements for the humane treatment of laboratory (experimental) animals. It also meets the international standard ISO 10993-1:2018, “Biological evaluation of medical devices—Part 1: Evaluation and testing within a risk management process” [23], and ISO 10993-2:2022, “Biological evaluation of medical devices—Part 2: Animal welfare requirements” [24].

**Informed Consent Statement:** Not applicable.

**Data Availability Statement:** The original contributions presented in this study are included in the article/Supplementary Material. Further inquiries can be directed to the corresponding author.

**Conflicts of Interest:** Author P.B. was an independent researcher affiliated with the University of Palermo (Palermo, Italy). Author D.N. served as the Deputy Director General for Research and Development at the Russian Office of APTOS LLC (Moscow, Russia). The remaining authors declare that the research was conducted in the absence of any commercial or financial relationships that could be construed as a potential conflict of interest. The authors also declare that this study received the institutional doctoral fund PJ\_DR\_D24\_INCR10\_37\_523976\_BURKO from the University of Palermo (Palermo, Italy), which supported the logistical needs of P.B. Additionally, this project utilized a research fund from APTOS LLC (Tbilisi, Georgia), which covered the project costs. Author G.S. was responsible for allocating this fund according to the project's budgetary needs. The funder was not involved in the study design, data collection, analysis, interpretation, the writing of this article, or the decision to submit it for publication.

## References

1. Su, D.; Wang, S.; He, T.; Wang, J. Experimental investigation of biostimulatory effects after polydioxanone thread insertion in a pig model. *J. Cosmet. Dermatol.* **2024**, *23*, 658–665. [[CrossRef](#)]
2. Niu, Z.; Zhang, K.; Yao, W.; Li, Y.; Jiang, W.; Zhang, Q.; Troulis, J.M.; August, M.; Chen, Y.; Han, Y. A meta-analysis and systematic review of the incidences of complications following facial thread-lifting. *Aesthetic Plast. Surg.* **2021**, *45*, 2148–2158. [[CrossRef](#)] [[PubMed](#)]
3. Yi, K.-H.; Park, S.Y. Facial thread lifting complications. *J. Cosmet. Dermatol.* **2025**, *24*, e16745. [[CrossRef](#)] [[PubMed](#)]
4. Beiu, C.; Popa, L.G.; Bălăceanu-Gurău, B.; Iliescu, C.A.; Racoviță, A.; Popescu, N.M.; Mihai, M.M. Personalization of minimally-invasive aesthetic procedures with the use of ultrasound compared to alternative imaging modalities. *Diagnostics* **2023**, *13*, 3512. [[CrossRef](#)] [[PubMed](#)]
5. Wortsman, X.; Wortsman, J. Sonographic outcomes of cosmetic procedures. *Am. J. Roentgenol.* **2011**, *197*, W910–W918. [[CrossRef](#)] [[PubMed](#)]
6. Samizadeh, S.; Samizadeh, S. Thread Types and Materials. In *Thread Lifting Techniques for Facial Rejuvenation and Recontouring*, 1st ed.; Samizadeh, S., Ed.; Springer: Cham, Switzerland, 2024; pp. 179–198.
7. Yongtrakul, P.; Sirithanabadeekul, P.; Siriphan, P. Thread lift: Classification, technique, and how to approach to the patient. *World Acad. Sci. Eng. Technol.* **2016**, *10*, 558–566.
8. De PinhoTavares, J.; Oliveira, C.A.C.P.; Torres, R.P.; Bahmad, F.J. Facial Thread Lifting with Suture Suspension. *Braz. J. Otorhinolaryngol.* **2017**, *83*, 712–719.
9. Park, J.H.; Lee, B.K.; Park, S.H.; Kim, M.G.; Lee, W.J.; Lee, Y.H.; Lee, B.H.; Kim, H.J.; Kim, S.M. Preparation of biodegradable and elastic poly( $\epsilon$ -caprolactone-co-lactide) copolymers and evaluation as a localized and sustained drug delivery carrier. *Int. J. Mol. Sci.* **2017**, *18*, 671. [[CrossRef](#)]
10. Samizadeh, S.; Samizadeh, S.; Sulamanidze, G.; Albina, K.; Sulamanidze, K.; Sulamanidze, M. P(LA/CL)-l-Poly lactide- $\Sigma$ -Caprolactone Threads—APTOS Threads: APTOS Solution—APTOS Methods and Threads. In *Thread Lifting Techniques for Facial Rejuvenation and Recontouring*, 1st ed.; Samizadeh, S., Ed.; Springer: Cham, Switzerland, 2024; pp. 223–235.
11. Zhang, M.; Chang, Z.; Wang, X.; Li, Q. Synthesis of poly(l-lactide-co- $\epsilon$ -caprolactone) copolymer: Structure, toughness, and elasticity. *Polymers* **2021**, *13*, 1270. [[CrossRef](#)] [[PubMed](#)]
12. Jelonek, K.; Kasperczyk, J.; Li, S.; Dobrzynski, P.; Janeczek, H.; Jarzabek, B. Novel poly(L-lactide-co- $\epsilon$ -caprolactone) matrices obtained with the use of Zr[Acac]<sub>4</sub> as nontoxic initiator for long-term release of immunosuppressive drugs. *Biomed. Res. Int.* **2013**, *2013*, 607351. [[CrossRef](#)] [[PubMed](#)]
13. Wong, V. The science of absorbable poly(L-lactide-co- $\epsilon$ -caprolactone) threads for soft tissue repositioning of the face: An evidence-based evaluation of their physical properties and clinical application. *Clin. Cosmet. Investig. Dermatol.* **2021**, *14*, 45–54. [[CrossRef](#)] [[PubMed](#)]
14. Berardesca, E.; Cirillo, P.; Fundaro, S.P.; Hau, K.C.; Moon, H.J.; Salti, G.; Goh, C.L.; Lao, P.P.; Savoia, A.; Coleman, S.R.; et al. *Reshaping with Barbed Threads*; Minerva Medica: Torino, Italy, 2020.
15. Liao, Z.-F.; Yang, W.; Li, X.; Wang, S.-W.; Liu, F.-C.; Luo, S.-K. Infraorbital rejuvenation combined with thread-lifting and non-cross-linked hyaluronic acid injection: A retrospective, case-series study. *Aesthetic Plast. Surg.* **2024**, *48*, 1589–1596. [[CrossRef](#)] [[PubMed](#)]
16. Liao, Z.-F.; Yang, W.; Lin, F.-C.; Wang, S.-W.; Hong, W.-J.; Luo, S.-K. A case study: Comprehensive approach for treating horizontal neck wrinkles using hyaluronic acid injections and thread-lifting. *Aesthetic Plast. Surg.* **2023**, *47*, 765–771. [[CrossRef](#)] [[PubMed](#)]
17. Sulamanidze, M.A.; Nikishin, D.V.; Sulamanidze, G.M.; Sulamanidze, K.M.; Kadzhaya, G.N. Method for Production of Medical Implant Shell, Medical Implant Shell. Russia Patent RU2782112C2, 21 October 2022.
18. Ziade, G.; Daou, D.; Karam, D.; Tsintsadze, M. The third generation barbed lifting threads: Added value of hyaluronic acid. *J. Cosmet. Dermatol.* **2024**, *23*, 186–192. [[CrossRef](#)] [[PubMed](#)]
19. Fernández, J.; Etxeberria, A.; Sarasua, J.-R. Synthesis, structure and properties of poly(L-lactide-co- $\epsilon$ -caprolactone) statistical copolymers. *J. Mech. Behav. Biomed. Mater.* **2012**, *9*, 100–112. [[CrossRef](#)] [[PubMed](#)]

20. Greco, R.M.; Iocono, J.A.; Ehrlich, H.P. Hyaluronic acid stimulates human fibroblast proliferation within a collagen. *Matrix. J. Cell. Physiol.* **1998**, *177*, 465–473. [[CrossRef](#)]
21. Dab, H.; Kacem, K.; Hachani, R.; Dhaouadi, N.; Hodroj, W.; Sakly, M.; Randon, J.; Bricca, G. Physiological regulation of extracellular matrix collagen and elastin in the arterial wall of rats by noradrenergic tone and angiotensin II. *J. Renin Angiotensin Aldosterone Syst.* **2012**, *13*, 19–28. [[CrossRef](#)] [[PubMed](#)]
22. Davison-Kotler, E.; Marshall, W.S.; García-Gareta, E. Sources of collagen for biomaterials in skin wound healing. *Bioengineering* **2019**, *6*, 56. [[CrossRef](#)] [[PubMed](#)]
23. *ISO 10993-1:2018; Biological Evaluation of Medical Devices—Part 1: Evaluation and Testing Within a Risk Management Process.* ISO: Geneva, Switzerland, 2018; p. 40.
24. *ISO 10993-2:2022; Biological Evaluation of Medical Devices—Part 2: Animal Welfare Requirements.* ISO: Geneva, Switzerland, 2022; p. 14.

**Disclaimer/Publisher’s Note:** The statements, opinions and data contained in all publications are solely those of the individual author(s) and contributor(s) and not of MDPI and/or the editor(s). MDPI and/or the editor(s) disclaim responsibility for any injury to people or property resulting from any ideas, methods, instructions or products referred to in the content.